

# Astragalus root induces ovarian $\beta$ -oxidation and suppresses estrogen-dependent uterine proliferation

BANZRAGCHGARAV ORKHON<sup>1</sup>, KYOKO KOBAYASHI<sup>1</sup>, BATKHUU JAVZAN<sup>2</sup> and KENROH SASAKI<sup>1</sup>

<sup>1</sup>Department of Pharmacognosy, Tohoku Medical and Pharmaceutical University, Sendai, Miyagi 981-8558, Japan;

<sup>2</sup>School of Engineering and Applied Sciences, National University of Mongolia, Ulaanbaatar 14201, Mongolia

Received October 23, 2017; Accepted March 26, 2018

DOI: 10.3892/mmr.2018.9493

**Abstract.** Continuous estrogen stimulation in the uterus has been known to cause excess proliferation of the functional layer of endometrium, resulting in endometrial hyperplasia and leading to infertility. Estrogens can modulate other nuclear receptor signaling pathways, such as peroxisome proliferator-activated receptors (PPARs). Astragalus root (AsR) has exhibited strong PPAR $\alpha$  agonistic activity. Female Imprinting Control Region mice were fed a powder diet that included 5% AsR hot water extract or 0.1% bezafibrate as a positive control for 56 days to investigate AsR effects on the reproductive tract, ovary and uterus. AsR resulted in upregulation of the expression of uterine and ovarian PPAR $\alpha$  mRNA by 2.5-fold, and 1.5-fold, respectively, compared with controls. AsR significantly increased ovarian expression levels of mitochondrial 2,4-dienoyl-CoA reductase (mDECR), an auxiliary enzyme involved in  $\beta$ -oxidation. AsR-fed mice also exhibited a significant increase in blood estradiol levels and tended to have higher ovary weight. AsR resulted in significantly decreased uterine weight and mDECR expression levels. It has been reported that a PPAR $\alpha$  agonist suppresses the development of estrogen-dependent endometrial hyperplasia. These findings raise the possibility that AsR suppresses estrogen-dependent endometrial hyperplasia and ovarian dysfunction leading to infertility.

## Introduction

The uterine menstrual cycle consists of four consecutive phases: Menstrual, proliferative, secretory, and ischemic. During the uterine proliferative phase, the thickness of the endometrium increases as a result of stimulation by estrogen produced by the ovaries. Continuous estrogen stimulation of the uterus has been known to cause excess proliferation of the

functional layer of the endometrium, which proceeds to the development of endometrial hyperplasia or atypical endometrial hyperplasia (1), leading to infertility. Estrogen, as well as epidermal growth factor (EGF) and transforming growth factor (TGF)  $\alpha$ , are involved in the proliferation of the endometrium. In normal and hyperplastic endometria, endometrial glands positive for TGF $\alpha$  are generally positive for estrogen receptor  $\alpha$  (ER $\alpha$ ) (2).

Peroxisome proliferator-activated receptors (PPARs) are members of the nuclear hormone receptor family. They are ligand-induced transcription factors that regulate the transcription of target genes. PPAR $\alpha$ , which is highly expressed in hepatocytes, cardiomyocytes, enterocytes, and kidney proximal tubule cells, is moderately expressed in the uterine glands, cervix (3,4) and ovarian follicular cells (4,5). ER $\alpha$ , a nuclear receptor, is activated by estrogens secreted from follicular lutein cells and binds to estrogen response elements (EREs) in the promoters of target genes involved in proliferation of the endometrium functional layer (6). Estrogens can modulate other nuclear receptor signaling pathways, such as that of PPARs (7). ER $\alpha$  binds to the peroxisome proliferator response element (PPRE) to interact with the ERE of the genes, and this transactivation by ER $\alpha$  is inhibited by PPARs through competition for ERE binding (8).

*Astragalus mongholicus* var. *membranaceus* Bunge. (synonym *A. membranaceus*) belongs to the family Leguminosae and is distributed throughout Mongolia, Russia, Kazakhstan, China, Japan, and Korea. The roots of *A. mongholicus*, which is used as a traditional medicine in Japan, is a part of *Kampo* medicine and indicated for tonic, cardiogenic, hydroschesis, diuresis, and hypotensive effects. The root has been reported to possess a wide range of various biological activities, such as anti-inflammatory properties (9), antiviral activity, immune modulation, antineoplastic activity, enhancement of cardiovascular function (10), anti-tumor activity (11). Chemical constituents have studied a lot, and main compounds are determined as astragalosides (12,13) and isoflavones (14). Astragaloside IV reduces A $\beta$  production in Alzheimer's disease (15) and has anticancer activities in breast cancer (16), hepatic cancer (17), and lung cancer (18).

In our previous report, a water extract of Astragalus root (AsR) exhibited PPAR $\alpha$  ligand activity, and AsR decreased renal fatty acid level through PPAR $\alpha$  expressed in proximal tubular epithelial cells, suggesting that AsR prevents renal

---

*Correspondence to:* Professor Kyoko Kobayashi, Department of Pharmacognosy, Tohoku Medical and Pharmaceutical University, 4-4-1 Komatsushima, Aoba, Sendai, Miyagi 981-8558, Japan  
E-mail: k-kyoko@tohoku-mpu.ac.jp

**Key words:** Astragalus root, PPAR $\alpha$ , ER $\alpha$ ,  $\beta$ -oxidation, ovary, uterus, anti-proliferation

damage by fatty acid overload (19). Therefore, we performed an experiment using mice to determine whether AsR has the likelihood of improving the function of the reproductive organs through its PPAR $\alpha$  agonistic activity.

## Materials and methods

*Extract of crude drug for PPAR $\alpha$  ligand test.* All crude drugs were purchased from Tochimoto Tenkaidou Co., Ltd. (Osaka, Japan). Each crude drug was refluxed for 1 h with 5-fold methanol. The solution was filtered, and the solvent was removed in a rotary evaporator (EYELA N-1100; Tokyo Rikakikai Co., Ltd., Tokyo, Japan) under reduced pressure to obtain the methanol extract.

*PPAR $\alpha$  agonistic activity by enzyme-linked immunosorbent assay (ELISA).* PPAR $\alpha$  agonistic activity was measured by an ELISA kit (Enbio RCAS for PPAR $\alpha$ ; Fujikura Kasei Co., Ltd., Ibaraki, Japan) according to the manufacturer's protocol. The ligand activity was calculated as  $(A-C)/(B-C) \times 100$ , where A is the absorbance of the sample, B is the absorbance of the positive control (0.5 mM bezafibrate), and C that of the blank (no sample).

*Comparison among PPAR $\alpha$ , PPAR $\gamma$  and ER $\alpha$  agonistic activities by ELISA.* Bezafibrate (Wako Pure Chemical Industries, Ltd., Osaka, Japan),  $\beta$ -estradiol (Wako Pure Chemical Industries, Ltd.), formononetin (Tokyo Chemical Industry Co., Ltd., Tokyo, Japan), astragaloside IV (Carbosynth Ltd., Berkshire, UK) were used for ELISA. Cyclic AMP response element binding protein (CRBP) binding protein (CBP; Bioss Antibodies, Woburn, MA, USA) was immobilized in the plastic wells at 4°C for 24 h. After washing the wells, 3% skim milk was added to each well as a blocking reagent. The sample solution, antigen (PPAR $\alpha$ , human recombinant, Fujikura Kasei Co., Ltd.; PPAR $\gamma$ , human recombinant; Prospec-Tany TechnoGene Ltd., Ness-Ziona, Israel), antibody (PPAR $\alpha$ , rabbit polyclonal, GeneTex Inc., Irvine, CA, USA; PPAR $\gamma$ , rabbit polyclonal, Bio-Rad Laboratories, Inc., Hercules, CA, USA; ER $\alpha$ , rabbit polyclonal; Signalway Antibody LLC, College Park, MD, USA) and IgG antibody conjugated alkaline phosphatase (PPAR $\alpha$  and ER $\alpha$ , Human IgG; Bethyl Laboratories, Inc., Montgomery, TX, USA; PPAR $\gamma$ , Rabbit IgG; Bio-Rad Laboratories, Inc.) were added to an individual well and incubated for 60 min at 37°C. Uterus of 13-week-old female ICR strain mice was used as a source of ER $\alpha$ . The supernatant of homogenized uterus in phosphate-buffered saline (PBS) was measured the total amount of protein by a protein assay kit (TaKaRa BCA Protein Assay kit; Takara Bio, Inc., Otsu, Japan), and 1  $\mu$ g protein was added to each well. After washing the wells, *p*-nitrophenyl phosphate (SIGMAFAST™ *p*-nitrophenyl phosphate tablets; Sigma-Aldrich; Merck KGaA, Darmstadt, Germany) was used as the substrate for alkaline phosphatase to develop color. After shaking the plate in a dark place, the absorbance of the solution in each well was measured at 405 nm. When the absorbance of the sample well was greater than that of the control well (without addition of extracts), the sample was deemed to have the agonistic activities.

*Extract of A. mongholicus root for animal test.* *A. mongholicus* root was purchased from Tochimoto Tenkaidou Co., Ltd.

The dried, chopped-root (5.0 g) was boiled in 600 ml distilled water, and the final volume reduced by half. The solution was filtered and concentrated in a rotary evaporator under reduced pressure at 40°C and then freeze-dried. The extract was stored at 4°C until use. The yield of the extract was  $1.49 \pm 0.13/5.0$  g of the chopped root.

*Animals.* Female SPF/ICR mice were purchased from Charles River Laboratories, Japan Inc. (Yokohama, Japan), and housed and maintained under standardized conditions of temperature ( $25 \pm 1^\circ\text{C}$ ) and humidity ( $55 \pm 5\%$ ) in a light cycle room (light from 07:00 a.m. to 07:00 p.m.; dark from 07:00 p.m. to 07:00 a.m.). The mice were allowed to acclimatize for a week. All experiments were approved by The Animal Experimental Committee of Tohoku Medical and Pharmaceutical University, and experimental procedures were conducted in accordance with the ethical guidelines of the University.

Female 13-week-old adult mice were divided randomly into three groups, with five mice in each group. The control, AsR and bezafibrate groups were fed a standard powdered chow (CE-2; CLEA Japan Inc., Tokyo, Japan) or chow containing 5% AsR or 0.1% bezafibrate (Wako Pure Chemical Industries, Ltd.) for 56 days. The body weight and food intake were measured randomly. Blood samples were collected from the tail vein and centrifuged at 6,000  $\times$  g for 10 min to obtain sera. Visceral adipose tissue (VAT), mammary glands, uterus, ovary and liver were collected after euthanasia by ether anesthesia. These tissues were weighed, and the tissues of on day 56 were prepared for measurements.

Female 20-week-old adult mice ( $n=5$ ) were treated with subcutaneous injection of 17 $\beta$ -estradiol at a dose of 0.5 mg/kg body weight once-daily for eight days. When mice were 21 weeks old, blood samples were collected from the tail vein and centrifuged at 6,000  $\times$  g for 10 min to obtain sera. Uteri and ovaries were collected after euthanasia by ether anesthesia. These tissues were weighed and prepared for each measurement.

*Quantitative analysis of PPAR $\alpha$  mRNA.* Total RNA and mRNA extraction, reverse transcription and real-time PCR were performed using kits and according to the manufacturers' protocols. Total RNA was extracted using Nucleo Spin RNA kit (Macherey-Nagel GmbH & Co. KG, Düren, Germany). mRNA was isolated from total RNA using the Oligotex-dT30 <Super> mRNA Purification kit (Takara Bio, Inc.). The mRNA was reverse-transcribed using Reverse transcription-PrimeScript RT reagent kit with gDNA Eraser (Takara Bio, Inc.), and cDNA was generated. To quantify PPAR $\alpha$ -mRNA expression, the synthesized cDNA fragments were amplified using Premix Ex Taq (Takara Bio, Inc.), and primers and probes for PPAR $\alpha$  (assay ID, Mm00440939\_m1) and GAPDH (assay ID, Mm99999915\_g1), used as an internal control in TaqMan Gene Expression Assays (Applied Biosystems; Thermo Fisher Scientific, Inc., Waltham, MA, USA), were used for qPCR. The qPCR conditions were as follows: Premix Ex Taq (probe qPCR, 2X conc.), 10  $\mu$ l; Taqman gene expression assay (premixing primer and probe, 20X conc.), 1  $\mu$ l; ROX reference dye (50X conc.), 0.4  $\mu$ l; sample, 2.0  $\mu$ l; dH $_2$ O, 6.6  $\mu$ l. qPCR was performed on a StepOnePlus Real-Time PCR system (Applied Biosystems; Thermo Fisher Scientific, Inc.) with the following PCR cycling

Table I. PPAR $\alpha$  agonistic activities of crude drugs.

Crude drug name	Representative of original plant source	Yield of extract (mg/g)	PPAR $\alpha$ ligand activity (%)
Astragalus Root	<i>Astragalus mongholicus</i>	20.0	83.45 $\pm$ 4.88
Zinger	<i>Zingiber officinale</i>	69.9	82.46 $\pm$ 11.03
Saposhnikovia Root and Rhizome	<i>Saposhnikovia divaricata</i>	9.6	73.64 $\pm$ 8.37
Sinomenium Stem and Rhizome	<i>Sinomenium acutum</i>	23.3	72.87 $\pm$ 15.10
Cnidium Rhizome	<i>Cnidium officinale</i>	174.5	63.83 $\pm$ 20.82
Japanese Angelica Root	<i>Angelica acutiloba</i>	63.1	63.45 $\pm$ 11.99
Peony Root	<i>Paeonia lactiflora</i>	135.7	38.65 $\pm$ 3.98
Atractylodes Rhizome	<i>Atractylodes japonica</i>	75.5	34.54 $\pm$ 17.52
Schizonepeta Spike	<i>Schizonepeta tenuifolia</i>	78.5	27.67 $\pm$ 5.63
Jujube	<i>Zizyphus jujuba</i>	489.3	23.58 $\pm$ 3.14
Mentha Herb	<i>Mentha arvensis</i>	68.8	NA
Glycyrrhiza	<i>Glycyrrhiza uralensis</i>	169.6	NA
Rhubarb	<i>Rheum palmatum</i>	298.2	NA
Scutellaria Radix	<i>Scutellaria baicalensis</i>	92.0	NA
Ephedra Herb	<i>Ephedra sinica</i>	88.4	NA
Bezafibrate		-	78.18 $\pm$ 2.97

Reaction concentration of methanol extract; 0.56 mg/ml, bezafibrate; 0.5 mM. Each value represented the average  $\pm$  standard deviation ( $n=3$ ); NA, no agonistic activity; PPAR, peroxisome proliferator-activated receptor.

conditions: Holding stage, 20 sec. 95°C; cycling stage, 40X (1 sec 95°C, 20 sec 60°C). The data was analyzed by comparative Cq method using StepOne Software version 2.3 (Applied Biosystems; Thermo Fisher Scientific, Inc.). The expression level of PPAR $\alpha$ -mRNA was represented by  $2^{-\Delta\Delta Cq}$  (20).

**Blood estradiol level.** Estradiol concentrations in sera were determined according to the manufacturer's protocol using the Estradiol EIA Kit (Diagnostic Systems Laboratories, Inc., Webster, TX, USA).

**Expression level of PPAR $\alpha$ , ER $\alpha$  and mitochondrial 2,4-dienoyl-CoA reductase (mDECR).** PPAR $\alpha$ , ER $\alpha$  and mDECR expression levels were checked by ELISA using 96-well plastic plates. The uterus, ovary and liver were homogenized in PBS (uterus: 75 mg/ml; ovary: 10 mg/ml; liver: 100 mg/ml) and centrifuged at 13,000  $\times$  g for 15 min at 4°C to obtain supernatants. The supernatant was measured the total amount of protein by a protein assay kit (TaKaRa BCA Protein Assay kit; Takara Bio, Inc.). ELISA was performed as follows. The supernatant was immobilized in each well at 37°C for 1 h after cAMP response element binding protein (CRBP; Bioss Antibodies) had been immobilized at 4°C for 24 h. 3% skim milk was used as blocking reagent, and Rabbit anti-human polyclonal PPAR $\alpha$  antibody (1:500, 44509; GeneTex Inc.), Rabbit polyclonal ER $\alpha$  antibody (1:500, 11071; Signalway Antibody LLC) or Rabbit anti-human polyclonal DECR1 antibody (1:500, 109608; GeneTex Inc.) was immobilized at 37°C for 1 h as the primary antibody. Goat anti-human polyclonal ALP-conjugated IgG (1:40, A80-219AP; Bethyl Laboratories, Inc.) or Goat anti-rabbit polyclonal ALP-conjugated IgG (1:40, 170-6518; Bio-Rad Laboratories Inc.) was used as a secondary

antibody. *p*-Nitrophosphate (Sigma-Aldrich; Merck KGaA) was used as a color reagent and 0.1 M EDTA as a stop reagent. Absorbance was measured at 405 nm. PPAR $\alpha$ , ER $\alpha$  and mDECR expression levels were represented as a relative ratio of the absorbance compared with the control group.

**Statistical analysis.** All data are expressed as the mean  $\pm$  standard deviation. The Mann-Whitney U test and ANOVA (Dunnett's test) were performed using the SigmaStat version 2.03 (Systat Software, Inc., San Jose, CA, USA).  $P < 0.05$  was considered to indicate a statistically significant difference.

## Results

**PPAR $\alpha$  agonistic activity of crude drugs.** As shown in Table I, a methanol extract of AsR had the strongest PPAR $\alpha$  agonistic activity among the 15 crude drugs.

**Comparison among PPAR $\alpha$ , PPAR $\gamma$  and ER $\alpha$  agonistic activities.** PPAR $\alpha$  agonistic activity of AsR was stronger than PPAR $\gamma$  agonistic activity, and AsR had weak agonistic activity on ER $\alpha$  (Fig. 1A). Bezafibrate showed significantly strong potent ER $\alpha$  agonistic activity (Fig. 1B). Formononetin and astragaloside IV, major ingredients in AsR, were compared with their PPAR $\alpha$  agonistic activities. Formononetin showed PPAR $\alpha$  agonistic activity in a dose-dependent manner, bezafibrate showed significantly strong PPAR $\alpha$  agonistic activity (Fig. 1C).

**Body weight and cumulative food intake.** The mice fed bezafibrate and AsR-supplements had significantly lower body

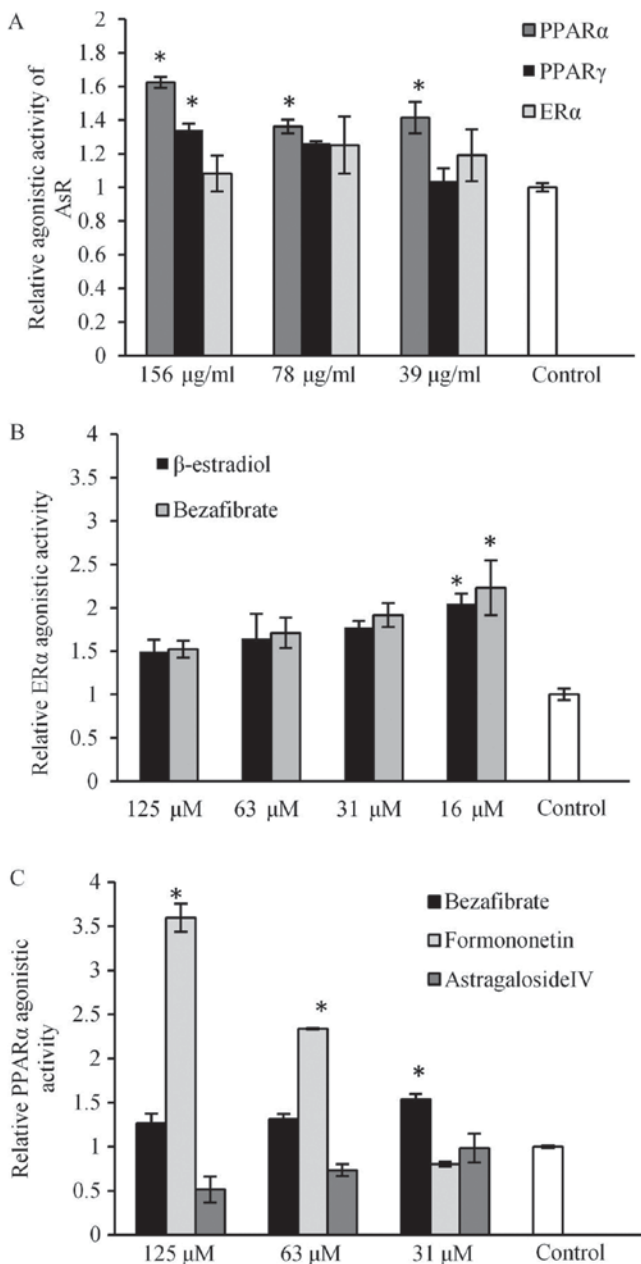


Figure 1. PPAR $\alpha$ , PPAR $\gamma$  and ER $\alpha$  agonistic activities. (A) Comparison of AsR agonistic activities among PPAR $\alpha$ , PPAR $\gamma$  and ER $\alpha$ . (B) ER $\alpha$  agonistic activities of bezafibrate and  $\beta$ -estradiol. (C) PPAR $\alpha$  agonistic activities of formononetin and astragaloside IV. \* $P < 0.05$ , one-way ANOVA performed after Dunnett's test. PPAR, peroxisome proliferator-activated receptor; AsR, Astragalus root; ER $\alpha$ , estrogen receptor  $\alpha$ .

weights compared to controls: AsR, at days 21, 27 and 33; bezafibrate, at day 33 (Fig. 2A). Across all the groups, no differences were observed in cumulative food intake from day 0 (Fig. 2B).

**Organ weight.** Mice with the bezafibrate treatment showed a trend toward decreased VAT weight (Fig. 3A) and mammary gland weight (Fig. 3B). Bezafibrate resulted in significantly higher liver weight on days 29 and 56 (Fig. 3C). Regarding the reproductive organs, the uterine weights decreased gradually during AsR treatment:  $160 \pm 29.05$ ,  $148.69 \pm 14.13$  and  $126.64 \pm 7.91$  mg at days 0, 29 and 56, respectively, but a

significant decrease was detected only on day 56 (Fig. 3D). The uterine weight of mice in the bezafibrate treatment group showed an increasing trend through the experiment. The uterine weight of estradiol-treated mice was significantly higher compared to the control group (Fig. 3D). Ovary weights tended to increase with AsR treatment (Fig. 3E).

**PPAR $\alpha$ -mRNA expression levels of organs.** We evaluated PPAR $\alpha$ -mRNA expression levels in the liver and reproductive organs using the comparative Ct method. The AsR group showed a trend toward increased the PPAR $\alpha$ -mRNA expression levels (by 2.51-fold) in the uterus (Fig. 5A) and significantly increased the PPAR $\alpha$ -mRNA expression levels (by 1.47-fold) in the ovary (Fig. 5B) compared to the control group. The bezafibrate group showed a trend toward increased the PPAR $\alpha$ -mRNA expression level in the uterus (Fig. 5A) and in the liver (Fig. 5C).

**Estradiol levels in serum.** In Fig. 6, blood-circulating estradiol levels in AsR-treated mice were significantly higher on day 21, and AsR showed an unstable increase of blood estradiol levels on day 29.

**ER $\alpha$  expression level in uterus.** The expression levels of uterine ER $\alpha$  were significantly lower in the AsR- and bezafibrate-treated groups (by approximately 42 and 55%, respectively) compared to the control group (Fig. 7A). In Fig. 7B, ER $\alpha$  expression levels per 0.5  $\mu$ g protein in the uterus were significantly increased in the AsR- and bezafibrate-treated groups compared with the control group.

**mDECOR expression levels in ovary and uterus.** The expression levels of ovarian mDECOR was significantly higher in the AsR-treated group (Fig. 8A). In Fig. 8B, mDECOR expression levels per 1.0  $\mu$ g protein in the ovary were significantly increased in AsR- and bezafibrate-treated groups. In the uterus, the mDECOR expression level was significantly lower in the AsR-treated group (Fig. 8C).

**Estradiol-treated mice.** The uterine weight of estradiol-treated mice was significantly higher compared to the control group (Fig. 4A). There is no effect on the ovary weight of estradiol-treated mice (Fig. 4B). Moreover, the expression levels in the uterus treated with estradiol was significantly lower compared to the control group (Fig. 4C). 17 $\beta$ -estradiol-treated mice had no effect to uterine ER $\alpha$  expression level (Fig. 4D).

## Discussion

**AsR influenced ovarian proliferation as a consequence of upregulation of mitochondrial  $\beta$ -oxidation.** Fatty acids provide acetyl-CoA through an enzyme-catalyzed reaction termed  $\beta$ -oxidation, which mainly occurs in mitochondria and to a lesser extent in peroxisomes. Saturated fatty acids are easily processed by  $\beta$ -oxidation, but unsaturated fatty acids are problematic for  $\beta$ -oxidation, and several auxiliary enzymes are required to generate conformations suitable for oxidation. Among these auxiliary enzymes, DECOR can process the unsaturated fatty acid trans-2-cis-4-dienoyl-CoA to

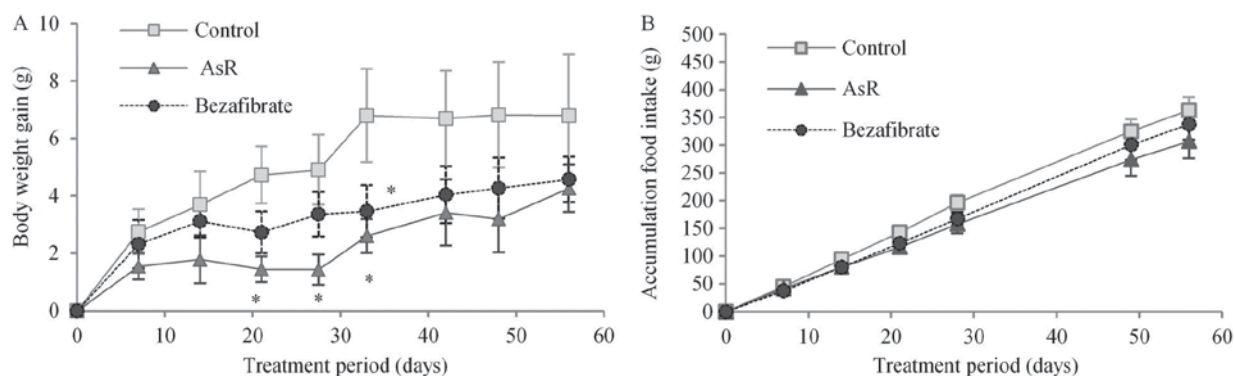


Figure 2. Monitoring body weight gain and cumulative food intake. (A) body weight gain; (B) cumulative food intake by treatment day. Each value represents the mean  $\pm$  SD (n=5). \*P<0.05, one-way ANOVA performed after Dunnett's test. AsR, Astragalus root.

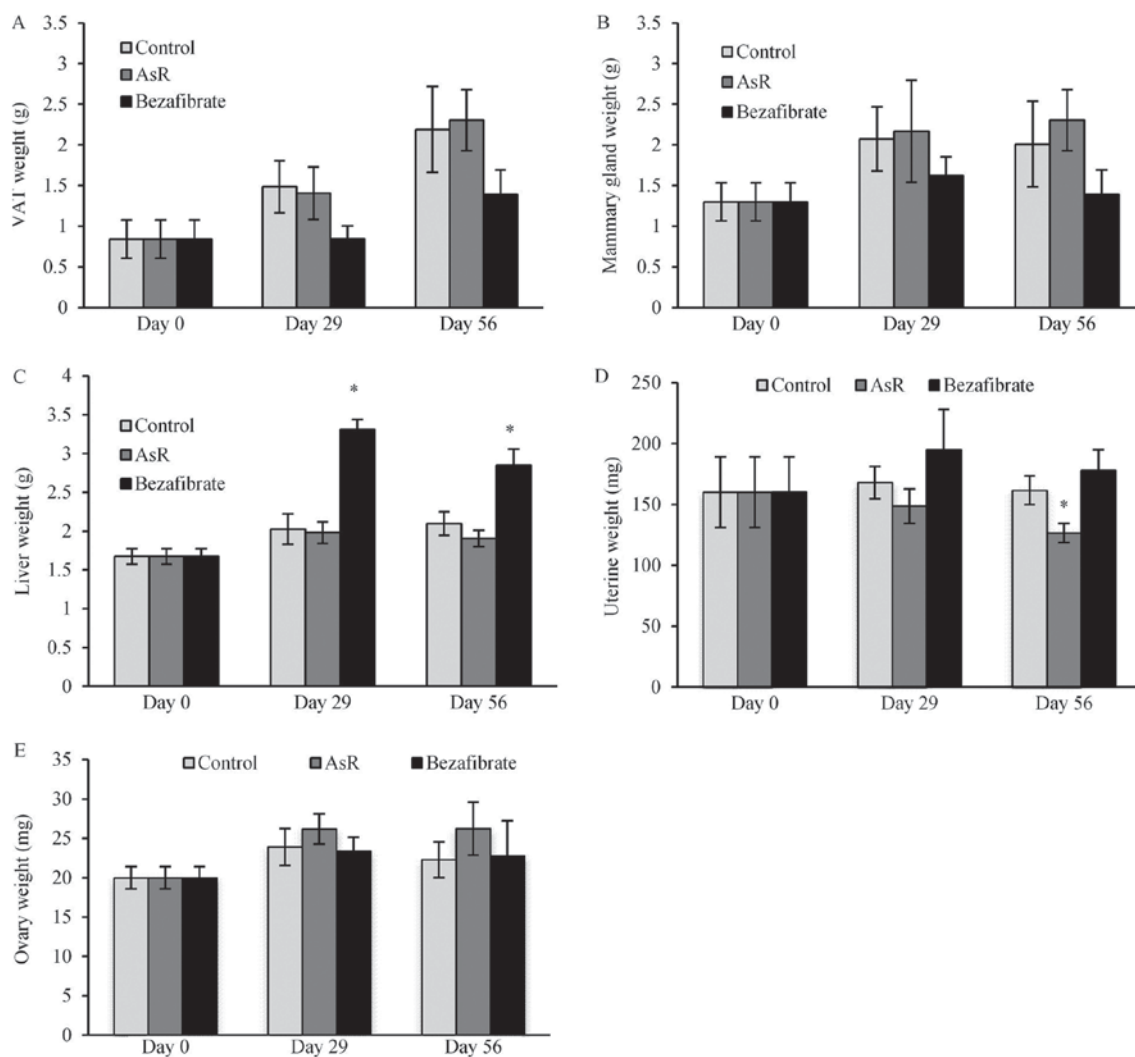


Figure 3. Wet organ weight. Weights of organs through treatment days. (A) VAT surrounding the uterus and ovaries; (B) mammary gland; (C) liver; (D) uterus; (E) ovary. Each value represents the mean  $\pm$  SD (n=5). \*P<0.05, one-way ANOVA performed after Dunnett's test. AsR, Astragalus root; VAT, visceral adipose tissue.

trans-3-enoyl-CoA, which is isomerized to a conformation suitable for  $\beta$ -oxidation. DECR activity is present in mitochondria and peroxisomes in mammals. There are two mitochondrial isoforms and at least one peroxisomal isoform of DECR in rats (21,22). AsR significantly increased the expression of

ovarian mDECR (Fig. 8A) in parallel with day-dependent increases of ovarian weight (Fig. 3E). The TCA cycle, which produces ATP as cell energy from acetyl-CoA provided by  $\beta$ -oxidation, is present in the mitochondria, but it is absent in the peroxisome. These findings suggest that AsR can produce

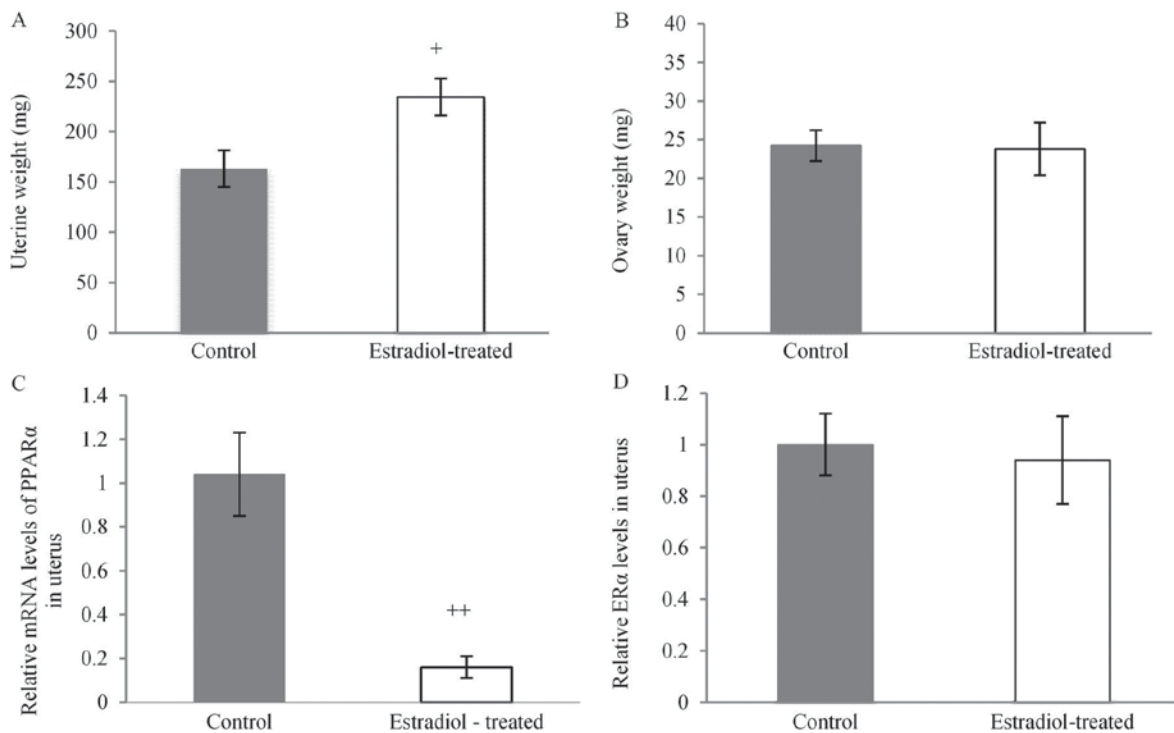


Figure 4. Influence of estradiol treatment on the reproductive organs. (A) uterine weight; (B) ovary weight; (C) PPAR $\alpha$ -mRNA expression levels in uterus; (D) ER $\alpha$  expression levels in uterus. The mice were injected with estradiol for 8 days at a dose of 0.5 mg/kg/day. Each value represents the mean  $\pm$  SD (n=5). \*P<0.05, \*\*P<0.01, Mann-Whitney U-test. PPAR, peroxisome proliferator-activated receptor; ER $\alpha$ , estrogen receptor  $\alpha$ .

cellular energy by increasing mitochondrial  $\beta$ -oxidation. Additionally, PPAR $\alpha$  expression levels increase during follicle development (23). AsR significantly increased the expression level of ovarian PPAR $\alpha$ -mRNA (Fig. 5B). AsR is thought to contribute to follicle development. Moreover, AsR significantly increased blood estradiol levels (Fig. 6). Estradiol-producing cells of the corpus luteum have three characteristic features: Lipid droplets, smooth endoplasmic reticulum and mitochondria, which contain the enzymes involved in the synthesis of estradiol. Follicle stimulating hormone (FSH) regulates estradiol secretion from ovaries, but mitochondria proliferation caused by increasing ovarian weight may be related to the amount of estradiol synthesis in the ovary.

Bezafibrate did not significantly affect ovarian PPAR $\alpha$ -mRNA expression levels or ovarian weight. Bezafibrate is known to strongly activate human PPAR $\alpha$ , whereas bezafibrate activates murine PPAR $\gamma$  twice as much as PPAR $\alpha$  (24). Bezafibrate-treated mice showed a trend toward a decrease in VAT and mammary gland weight. These data suggest that bezafibrate promotes white adipose differentiation by activating murine PPAR $\gamma$ . PPAR $\gamma$  agonistic activity of AsR was weaker than PPAR $\alpha$  agonistic activity *in vitro* (Fig. 1A) and AsR did not decrease VAT weight of mice. Therefore, AsR might have no effective agonistic activity for PPAR $\gamma$ . Bezafibrate increased ovarian mDECOR per protein amount (Fig. 8B), but did not affect to ovarian mass (Fig. 3E). PPAR $\gamma$  activation by bezafibrate may prevent ovarian proliferation.

Mitochondrial dysfunction has been implicated in cellular senescence in ovarian aging (25). AsR might improve ovarian dysfunction by upregulating mitochondrial  $\beta$ -oxidation and PPAR $\alpha$  expression.

*AsR attenuates the proliferative action of the uterus.* PPAR $\alpha$  forms heterodimers with retinoic X receptor (RXR), binds to PPREs in the promoter of target genes, and can bind to diverse hormone responsive elements, such as the ERE. ER $\alpha$  binds to the PPRE sequence to interact with ERE, and this transactivation by ER $\alpha$  is inhibited by PPARs/RXR through competition for binding to EREs (8). It has also been reported that PPAR $\alpha$  and ER $\alpha$  share the ability to bind to the AGGTCA half-site, which occurs as palindrome and as a direct repeat in ERE and PPRE sequences, respectively (26). Mice treated with estradiol by subcutaneous injection had significantly decreased expression of uterine PPAR $\alpha$ -mRNA (Fig. 4C). It is apparent that a negative cross-talk exists between PPAR $\alpha$  and ER $\alpha$  activation or expression, and hence increased uterine PPAR $\alpha$ -mRNA expression occurred in mice treated with AsR (Fig. 5A) resulted in diminished uterine ER $\alpha$  expression levels (Fig. 7A). ER $\alpha$  is needed for complete EGF response leading to proliferation of the endometrium, and ER $\alpha$  has been observed in the endometrium of endometriosis patients (27). Fenofibrate, PPAR $\alpha$  agonist, was reported that it was influenced to attenuate of the uterine weight (28). As shown in Fig. 7B, ER $\alpha$  expression level per 0.5  $\mu$ g protein in the uterus was significantly higher than that of control. Fenofibrate, a PPAR $\alpha$  agonist, are increased levels of ER $\alpha$  in randomly selected section of uterus accompanied by decreased in mitosis and cell proliferation in myometrial cells, stromal cells, glandular epithelium and luminal epithelium, and also increased  $\beta$ -catenin in glandular epithelium and luminal epithelium to protect from the formation of precancerous changes (28). AsR showed weak ER $\alpha$  agonistic activity and strong on PPAR $\alpha$  (Fig. 1A). It is thought that these agonistic activities by AsR might lead to a decrease of uterine mass. As shown in Fig. 9, AsR affects the molecular mechanism in

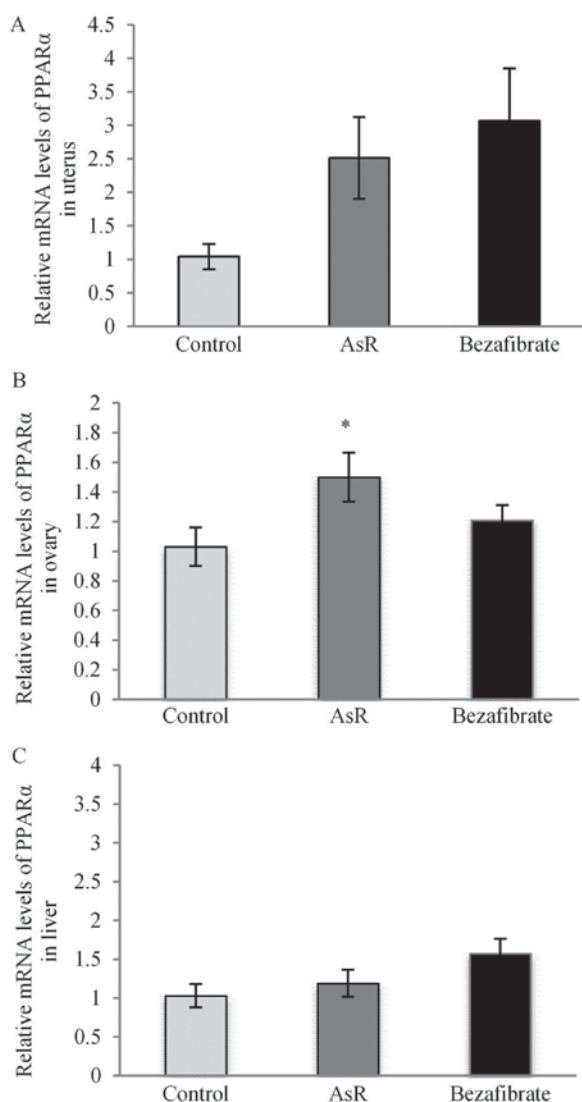


Figure 5. PPAR $\alpha$ -mRNA levels in each organ. PPAR $\alpha$ -mRNA expression levels in each organ on day 56. (A) uterus; (B) ovary; (C) liver. Each value represents the mean  $\pm$  SD (n=5). \*P<0.05, one-way ANOVA performed after Dunnett's test. PPAR, peroxisome proliferator-activated receptor; AsR, Astragalus root

PPAR $\alpha$  and ER $\alpha$ , AsR might prevent estrogen-dependent endometrial hyperplasia by downregulating ER $\alpha$  expression through its PPAR $\alpha$  agonistic activity and PPAR $\alpha$  proliferation.

Fig. 5A shows that bezafibrate treatment resulted in increased PPAR $\alpha$ -mRNA expression levels, but also resulted in a trend toward increased uterine weight (Fig. 3D). The PPAR $\gamma$  agonist rosiglitazone supports the development of estrogen-dependent endometrial hyperplasia, and increases the uterine weight because the PPAR $\gamma$  agonist enhances proliferative and morphogenetic estrogen action (28). Bezafibrate is thought to act on murine PPAR $\gamma$  in the uterus. AsR, on the other hand, showed PPAR $\gamma$  agonistic activity weaker than that of PPAR $\alpha$  (Fig. 1A). It is thought that AsR would activate more strongly to uterine PPAR $\alpha$  than PPAR $\gamma$ .

In our previous report, AsR increases the consumption of fatty acids through PPAR $\alpha$  expressed in PTECs (19). In ovary, AsR contributes the production of energy through the consumption of fatty acids in mitochondria. Conversely,

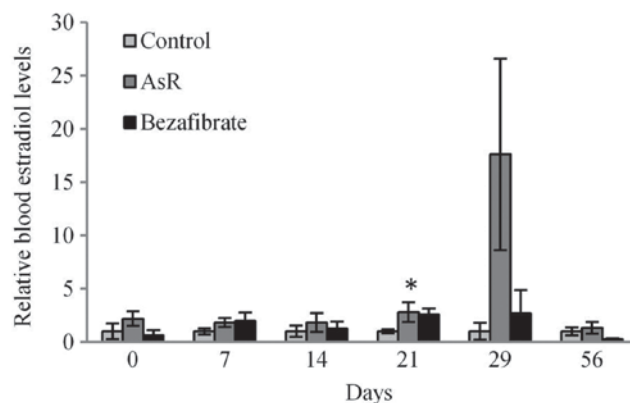


Figure 6. Influence on blood estrogen levels. Blood estrogen levels on treatment days. Each value represents the mean  $\pm$  SD (n=5). \*P<0.05, one-way ANOVA performed after Dunnett's test. AsR, Astragalus root.

AsR is not involved in the consumption of fatty acids in uterine mitochondria (Fig. 8C), suggesting that in the uterine decreased of the mass by PPAR $\alpha$  agonist were suppressed the energy production by mitochondria.

The diseases of endometrial hyperplasia (EH) and atypical endometrial hyperplasia (AEH) occur due to continuous estrogen-stimulation and continuous progesterone-reduction. AEH increases the risk of endometrial carcinoma, but EH is not associated with risk of endometrial carcinoma (29,30). As shown in Fig. 1C, formononetin that is one of the main constituents of AsR showed strong agonistic activity on PPAR $\alpha$ . Formononetin might prevent uterine proliferative action by continuous estrogen stimulation as a PPAR $\alpha$  activator and PPAR $\alpha$  proliferator. Moreover, AsR increases the secretion of estradiol caused by ovarian proliferation. Our findings raise the possibility that AsR is likely to contribute to the improvement of infertility caused by endometrial hyperplasia and ovarian dysfunction. In recent studies, oogonial stem cells promote ovarian regeneration and sustain ovarian function (31,32). In our research in progress, the ovariectomized mice fed a 10% AsR-included diet showed rearrangements of the ovary in 4 of 5 tested animals after exposure for 49 days. It is hoped that AsR may be used as regenerative medicine to treat women suffering from ovarian failure or extirpation.

## Acknowledgements

The authors would like to thank to all the members of JICA M-JEED project in Mongolia, B. Orkhon, a student on the doctoral course, obtained financial supports from this project. We also would like to thank Nobuyoshi Kadowaki and Moe Hayashi, undergraduates of Tohoku Medical and Pharmaceutical University, for their efforts in the animal experiments.

## Acknowledgements

Not applicable.

## Funding

No funding was received.

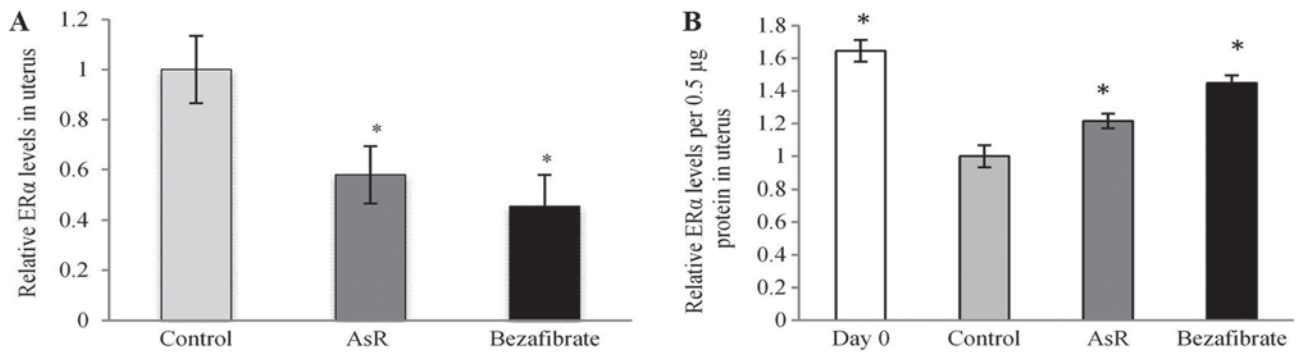


Figure 7. Influence on uterine ERα expression levels. (A) ERα expression levels in the uterus. (B) ERα expression levels per 0.5 μg protein in the uterus. Each value represents the mean ± SD (n=5). \*P<0.05, one-way ANOVA performed after Dunnett's test. AsR, Astragalus root; ERα, estrogen receptor α.

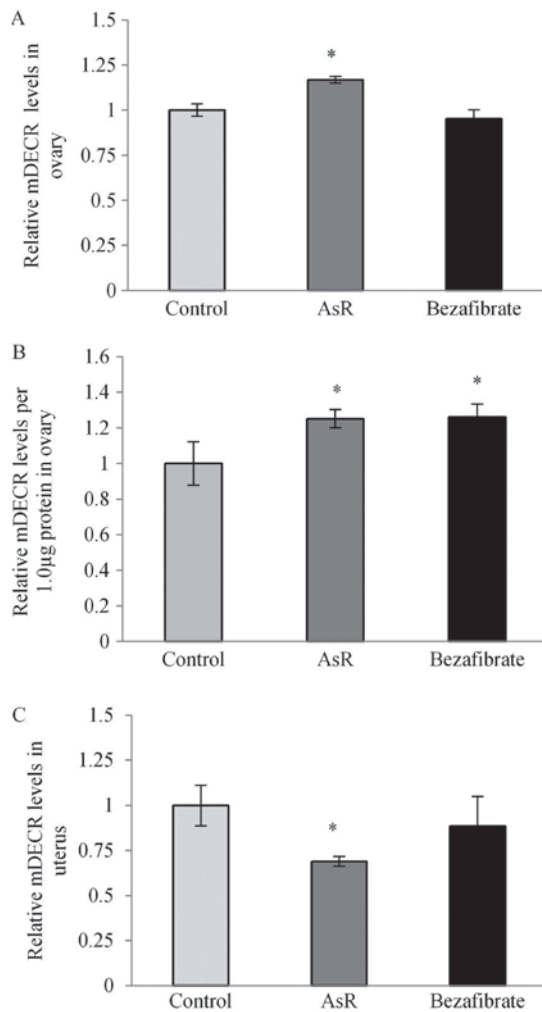


Figure 8. Influence on mDECR expression levels in the ovary and uterus. (A) mitochondrial DECR expression levels in the ovary. (B) mitochondrial DECR expression levels per 1.0 μg protein in the ovary. (C) mDECR expression levels in uterus. Each value represents the mean ± SD (n=5). \*P<0.05, one-way ANOVA performed after Dunnett's test. AsR, Astragalus root; mDECR, mitochondrial 2,4-dienoyl-CoA reductase.

**Availability of data and materials**

The datasets used and/or analyzed during current study are available from the corresponding author on reasonable request.

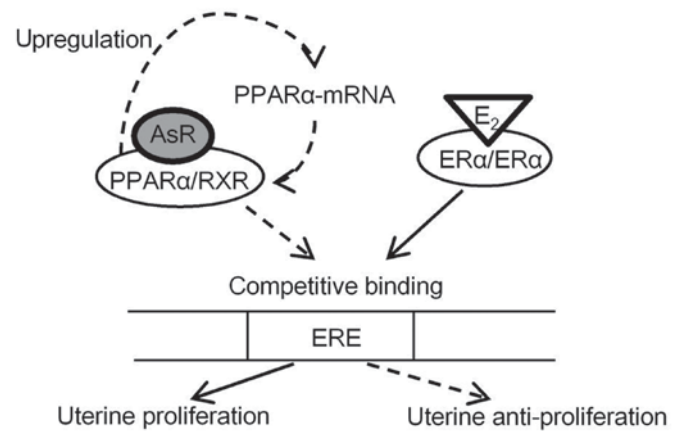


Figure 9. Molecular mechanism in PPARα and ERα. Estradiol (E2)-ERα complex promotes uterine proliferation through binding to ERE. AsR-PPARα complex upregulates PPARα gene transcription and promotes competitive binding with ERα to ERE. Accordingly, uterine anti-proliferation is induced by AsR-treatment. PPAR, peroxisome proliferator-activated receptor; AsR, Astragalus root; ERα, estrogen receptor α; ERE, estrogen response element.

**Authors' contributions**

BO analyzed and KK designed the research, analyzed the data and prepared the manuscript. BJ and KS contributed in guiding research and interpreting the data. All authors read and approved the final manuscript.

**Ethics approval and consent to participate**

All experiments were approved by The Animal Experimental Committee of Tohoku Medical and Pharmaceutical University, and experimental procedures were conducted in accordance with the ethical guidelines of the University.

**Consent for publication**

Not applicable.

**Competing interests**

The authors declare that they have no competing interests.

## References

- Llorens MA, Bermejo MJ, Salcedo MC, Charro AL and Puente M: Epidermal growth factor receptors in human breast and endometrial carcinomas. *J Steroid Biochem* 34: 505-509, 1989.
- Niikura H, Sasano H, Kaga K, Sato S and Yajima A: Expression of epidermal growth factor family proteins and epidermal growth factor receptor in human endometrium. *Hum Pathol* 27: 282-289, 1996.
- Houston KD, Copland JA, Broaddus RR, Gottardis MM, Fischer SM and Walker CL: Inhibition of proliferation and estrogen receptor signaling by peroxisome proliferator-activated receptor gamma ligands in uterine leiomyoma. *Cancer Res* 63: 1221-1227, 2003.
- Braissant O, Fougelle E, Scotto C, Dauça M and Wahli W: Differential expression of peroxisome proliferator-activated receptors (PPARs): Tissue distribution of PPAR-alpha, -beta, and -gamma in the adult rat. *Endocrinology* 137: 354-366, 1996.
- Zhao Y, Tan YS, Strynar MJ, Perez G, Haslam SZ and Yang C: Perfluorooctanoic acid effects on ovaries mediate its inhibition of peripubertal mammary gland development in Balb/c and C57Bl/6 mice. *Reprod Toxicol* 33: 563-576, 2012.
- Mitchell DC and Ing NH: Estradiol stabilizes estrogen receptor messenger ribonucleic acid in sheep endometrium via discrete sequence elements in its 3'-untranslated region. *Mol Endocrinol* 17: 562-574, 2003.
- Bonfiglioglio D, Gabriele S, Aquila S, Catalano S, Gentile M, Middea E, Giordano F and Andó S: Estrogen receptor alpha binds to peroxisome proliferator-activated receptor response element and negatively interferes with peroxisome proliferator-activated receptor gamma signaling in breast cancer cells. *Clin Cancer Res* 11: 6139-6147, 2005.
- Mu YM, Yanase T, Nishi Y, Takayanagi R, Goto K and Nawata H: Combined treatment with specific ligands for PPARgamma: RXR nuclear receptor system markedly inhibits the expression of cytochrome P450arom in human granulosa cancer cells. *Mol Cell Endocrinol* 181: 239-248, 2001.
- Wang QH, Han N, Dai N, Wang X and Ao W: Anti-inflammatory effects and structure elucidation of two new compounds from *Astragalus membranaceus* (Fisch) Bge. var. *mongholicus* (Bge) Hsiao. *J Mol Struct* 1074: 284-288, 2014.
- No authors listed: *Astragalus membranaceus*. Monograph. *Altern Med Rev* 8: 72-77, 2003.
- Chen J, Ge B, Wang Y, Ye Y, Zeng S and Huang Z: Biochanin A promotes proliferation that involves a feedback loop of microRNA-375 and estrogen receptor alpha in breast cancer cells. *Cell Physiol Biochem* 35: 639-646, 2015.
- Tohda C, Tamura T, Matsuyama S and Komatsu K: Promotion of axonal maturation and prevention of memory loss in mice by extracts of *Astragalus mongholicus*. *Br J Pharmacol* 149: 532-541, 2006.
- Kitagawa I, Wang HK, Saito M, Takagi A and Yoshikawa M: Saponin and sapogenol. XXXV. Chemical constituents of *Astragalus membranaceus* BUNGE. (2). Astragalosides I, II and IV, Acetylastragaloside I and isoastragalosides I and II. *Chem Pharm Bull* 31: 698-708, 1983.
- Luo HL, Zhong J, Ye FY, Wang Q, Ma YM, Liu P, Zhang H, Sunc MY and Jiang J: A systematic quality control method of Huangqi decoction: Simultaneous determination of eleven flavonoids and seven triterpenoid saponins by UHPLC-MS. *Anal Methods* 6: 4593-4601, 2014.
- Wang X, Wang Y, Hu JP, Yu S, Li BK, Cui Y, Ren L and Zhang LD: Astragaloside IV, a natural PPAR $\gamma$  agonist, reduces A $\beta$  production in Alzheimer's disease through inhibition of BACE1. *Mol Neurobiol* 54: 2939-2949, 2017.
- Jiang K, Lu Q, Li Q, Ji Y, Chen W and Xue X: Astragaloside IV inhibits breast cancer cell invasion by suppressing Vav3 mediated Rac1/MAPK signaling. *Int Immunopharmacol* 42: 195-202, 2017.
- Wang PP, Xu DJ, Huang C, Wang WP and Xu WK: Astragaloside IV reduces the expression level of P-glycoprotein in multidrug-resistant human hepatic cancer cell lines. *Mol Med Rep* 9: 2131-2137, 2014.
- Cheng X, Gu J, Zang M, Yuan J, Zhao B, Jiang J and Jia X: Astragaloside IV inhibits migration and invasion in human lung cancer A549 cells via regulating PKC- $\alpha$ -ERK1/2-NF- $\kappa$ B pathway. *Int Immunopharmacol* 23: 304-313, 2010.
- Kobayashi K, Matsuyama W, Arai Y, Koizumi S, Shimizu T, Tomioka R and Sasaki K: Boiogito increases the metabolism of fatty acids in proximal tubular cells through peroxisome proliferator-activated receptor (PPAR)  $\alpha$  agonistic activity. *Biol Pharm Bull* 39: 143-147, 2016.
- Livak KJ and Schmittgen TD: Analysis of relative gene expression data using real-time quantitative PCR and the 2<sup>- $\Delta\Delta$ Ct</sup> method. *Methods* 25: 402-408, 2001.
- Dommes V, Baumgart C and Kunau WH: Degradation of unsaturated fatty acids in peroxisomes. Existence of a 2,4-dienoyl-CoA reductase pathway. *J Biol Chem* 256: 8259-8262, 1981.
- Hakkola EH, Autio-Harmainen HI, Sormunen RT, Hassinen IE and Hiltunen JK: The known purified mammalian 2,4-dienoyl-CoA reductases are mitochondrial isoenzymes. *J Histochem Cytochem* 37: 1863-1867, 1989.
- Rak-Mardyła A and Drwal E: In vitro interaction between resistin and peroxisome proliferator-activated receptor  $\gamma$  in porcine ovarian follicles. *Reprod Fertil Dev* 28: 357-368, 2016.
- Willson TM, Brown PJ, Sternbach DD and Henke BR: The PPARs: From orphan receptors to drug discovery. *J Med Chem* 43: 527-550, 2000.
- Wang T, Zhang M, Jiang Z and Seli E: Mitochondrial dysfunction and ovarian aging. *Am J Reprod Immunol* 77: e12651, 2017.
- Keller H, Givel F, Perroud M and Wahli W: Signaling cross-talk between peroxisome proliferator-activated receptor/retinoid X receptor and estrogen receptor through estrogen response elements. *Mol Endocrinol* 9: 794-804, 1995.
- Dassen H, Punyadeera C, Delvoux B, Schulken I, Marchetti C, Kamps R, Klomp J, Dijcks F, de Goeij A, D'Hooghe T, et al: Olfactomedin-4 regulation by estrogen in the human endometrium requires epidermal growth factor signaling. *Am J Pathol* 177: 2495-2508, 2010.
- Gunin AG, Bitter AD, Demakov AB, Vasilieva EN and Suslonova NV: Effects of peroxisome proliferator activated receptors-alpha and -gamma agonists on estradiol-induced proliferation and hyperplasia formation in the mouse uterus. *J Endocrinol* 182: 229-239, 2004.
- Kurman RJ, Kaminski PF and Norris HJ: The behavior of endometrial hyperplasia. A long-term study of 'untreated' hyperplasia in 170 patients. *Cancer* 56: 403-412, 1985.
- Lindahl B and Willén R: Spontaneous endometrial hyperplasia. A prospective, 5 year follow-up of 246 patients after abrasio only, including 380 patients followed-up for 2 years. *Anticancer Res* 14: 2141-2146, 1994.
- Truman AM, Tilly JL and Woods DC: Ovarian regeneration: The potential for stem cell contribution in the postnatal ovary to sustained endocrine function. *Mol and Cell Endocrinol* 445: 74-84, 2017.
- Erler P, Sweeney A and Monaghan JR: Regulation of injury-induced ovarian regeneration by activation of Oogonial stem cells. *Stem Cells* 35: 236-247, 2017.